Materials Science & Engineering A 565 (2013) 321–325

Contents lists available at SciVerse ScienceDirect

Materials Science & Engineering A

journal homepage: www.elsevier.com/locate/msea

Compressive creep behavior of cast Bi_2Te_3

Zhi-Ping Guan [a], David C. Dunand [b,*]

[a] Superplastic & Plastic Research Institute, Jilin University, Changchun, Jilin 130022, China
[b] Department of Materials Science and Engineering, Northwestern University, Evanston, IL 60208, USA

ARTICLE INFO

Article history:
Received 16 November 2012
Received in revised form
7 December 2012
Accepted 19 December 2012
Available online 28 December 2012

Keywords:
Bismuth telluride
Deformation
Plasticity
Oxidation
Thermoelectric material

ABSTRACT

In thermoelectric devices, Bi_2Te_3 must be able to operate under high temperature gradients for very long times (years) without appreciable deformation, while being subjected to stresses created by internal thermal mismatch and external forces (e.g., vibrations). The deformation rate of cast, coarse-grained Bi_2Te_3 was measured under uniaxial compressive stresses from 2 to 16 MPa at temperatures between 400 and 500 °C. At all temperatures, a power-law behavior is observed, with a stress exponent $n=3$–6 and an activation energy of ~145 kJ/mol. Significant differences in creep rates are observed in duplicate experiments, which may be due to anisotropic creep resistance in coarse-grained specimens. Bi_2Te_3 is brittle at 400 and 450 °C but shows some compressive ductility at 500 °C, indicating that hot forging may be possible.

1. Introduction

Thermoelectric materials can produce electrical power in temperature gradients via the Seebeck effect and provide cooling capability via the Peltier effect [1]. Bi_2Te_3-based alloys are the most commercialized thermoelectric materials for applications, typically reaching a thermoelectric figure of merit, ZT, close to unity near room temperature. Thermoelectric devices based on Bi_2Te_3 and other compounds can be used for energy harvesting applications, for example, as independent power sources for sensor networks or in consumer electronics [2,3].

Bi_2Te_3 has a rhombohedral unit cell with atoms organized in Bi or Te planes with hexagonal packing [4]. Bonding between neighboring atoms and planes varies from strong covalent to covalent–ionic to weak van der Waals. As expected from this bonding structure, Bi_2Te_3 is brittle at ambient temperature [5]. But, like most brittle compounds, Bi_2Te_3 may become ductile at elevated temperature.

At the hot side of thermoelectric devices, Bi_2Te_3 is operating at a high homologous temperature T/T_m, where $T_m=858$ K (585 °C) is the absolute melting temperature of Bi_2Te_3. Creep deformation is thus of relevance for a device operating over many years and subjected to internal stresses (e.g., due to thermal mismatch with other members coupled mechanically to the thermoelectric materials, and/or from thermal expansion mismatch along the Bi_2Te_3 elements in a steady-state or transient temperature gradient) or to external stresses (e.g., during operation of devices in automotive environment from vibrations and shocks) [6–8]. This paper reports on the mechanical behavior of cast, coarse-grained Bi_2Te_3, during compressive creep experiments performed at 400, 450 and 500 °C for times ranging up to 146 h.

2. Experimental procedures

Bi_2Te_3 ingots were obtained from Sichuan Xinlong Tellurium Industry & Technique Development Co. (China) which reported a 99.99% purity. Coarse Bi_2Te_3 pieces (created by fracturing as-received ingots) were vacuum sealed within a quartz tube with internal diameter of ~7 mm and melted by heating to 600 °C at a rate of 7 °C/min. After holding the melt at 600 °C for 36 min while thoroughly shaking and mixing it, Ar gas was filled into the quartz tube up to an absolute pressure of 21 kPa in order to minimize pores (presumably created by slight Bi_2Te_3 decomposition) present in the liquid Bi_2Te_3. The material was slowly cooled in ~3 h to ambient temperature and creep specimens were cut from the solidified ingot with a diamond saw to a length of ~14 mm, resulting in cylinders with aspect ratio of ~2 and two parallel end surfaces.

Oxidation studies were carried out on samples with mass of ~4.1 g in laboratory air at 400, 450 and 500 °C over a time span of 200–500 h. The samples were placed in flat-bottom quartz tubes and removed from the furnace at increasing time intervals to be weighed within their quartz tubes which collected any spalled oxide.

Constant-load creep tests, with compressive stresses in the range of 2–16 MPa, were performed in air at 400 and 450 °C and

* Corresponding author. Tel.: +1 847 4915370; fax: +1 847 4676573.
E-mail address: dunand@northwestern.edu (D.C. Dunand).

0921-5093/$ - see front matter © 2013 Elsevier B.V. All rights reserved.
http://dx.doi.org/10.1016/j.msea.2012.12.052

under flowing Ar gas at 500 °C. A nickel-base superalloy creep cage translated tensile loads in the pull-rods to compressive stresses on the specimen. Frictional effects on the end-loaded specimens were minimized using alumina platens coated with boron nitride. Specimen temperature was measured in the three-zone furnace with a temperature stability of ±1 °C after a 1 h soak at the test temperature. Specimen strain was calculated from extensiometric displacements of cage platens measured using a linear variable differential transducer (LVDT) with a resolution of 2.5 μm. Once steady-state deformation was achieved, the load was increased, resulting in 3–5 data points suitable for determining stress exponent from a single specimen. Total specimen strain never exceeded 10%.

3. Results and discussion

3.1. Microstructure and oxidation behavior

Fig. 1 shows the microstructure of cast Bi_2Te_3. It consists of coarse, elongated grains with ~2–4 mm length and ~0.1–0.3 mm width with an interwoven arrangement similar to a basket-weave structure. Each grain appears to consist of many elongated subgrains, oriented in the same direction as that of the grain.

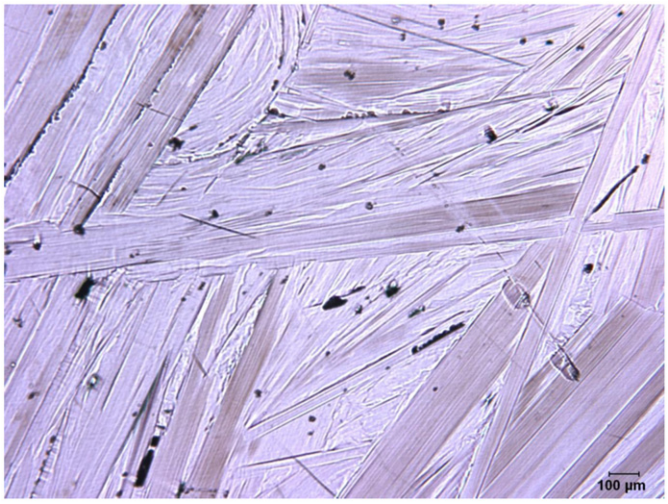

Fig. 1. Micrograph of polished cross-section of cast Bi_2Te_3.

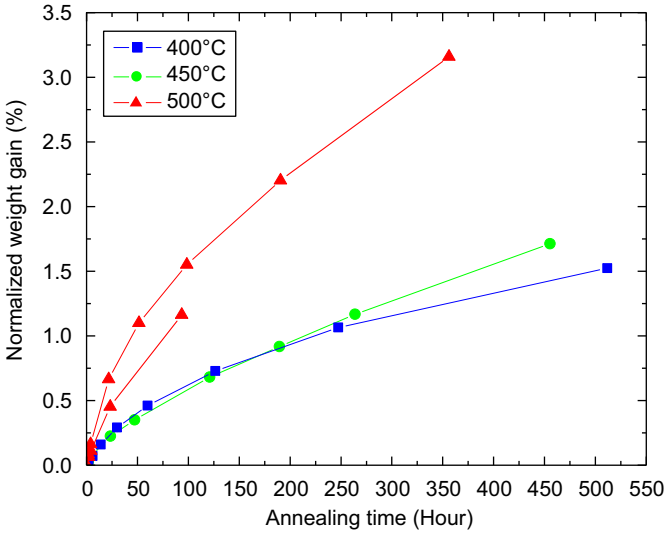

Fig. 2. Time dependence of mass gain due to oxidation in laboratory air of cast Bi_2Te_3 at 400, 450 and 500 °C.

Fig. 2 displays curves for the normalized weight gain vs. time at 400, 450 and 500 °C. The weight gain was caused by sample oxidation, and the surface of the samples was covered by white or bright yellow layers of mixed bismuth and tellurium oxides [9,10]. Additionally, there was a small weight loss by evaporation of tellurium, which was detected from a silvery-white deposit on the inner surface at the top of the quartz tube. Compared with the weight gain from oxidation, the weight loss from evaporation is very small and can be ignored.

From Fig. 2, it is apparent that the oxidation of Bi_2Te_3 during annealing at 500 °C is much faster than at 400 and 450 °C, whose rates are quite similar. Therefore, the compressive creep tests at 500 °C were carried out under flowing Ar to minimize sample oxidation while the creep tests at 400 and 450 °C were performed in air because the mass loss from oxidation was deemed negligible for the times used here.

3.2. Stress dependence of creep rate

Fig. 3 shows some of the creep curves at the three temperatures investigated. A primary creep regime, where the strain rate decreases continuously with time, always precedes steady-state creep. The strain associated with primary creep can be considerable (~0.5–1%) and stretch over long times (up to 25 h for the sample tested at 450 °C at 3.0 MPa), and represents the establishment of a steady-state dislocation glide structure within the grains.

In the secondary creep regime, a minimum strain rate was found, which is plotted as a function of applied stress in Fig. 4 for tests performed at 400, 450 and 500 °C. The data can be described by a power-law equation of the form [11]

$$\dot{\varepsilon} = A\sigma^n \exp\left(-\frac{Q}{R_g T}\right) \quad (1)$$

where $\dot{\varepsilon}$ is the minimum, secondary strain rate, A is a constant, σ is the applied stress, n is the stress exponent, Q is the activation energy for creep, R_g is the gas constant, and T is the absolute temperature. Fig. 4 shows stress exponents of n~4–6 at 400 °C, n~3 at 450 °C and n~4 at 500 °C. The value at 450 °C is very imprecise, as it was determined from only three data points. These stress exponents are in the same range as those for covalent elements (n=5 for Si and Ge), ionic compounds (n=3.6 for NaCl, 6.6 for LiF, 3.3 for MgO and 4.2 for FeO), and partially ionic compounds (n=5 for ZrC and TiC) [11].

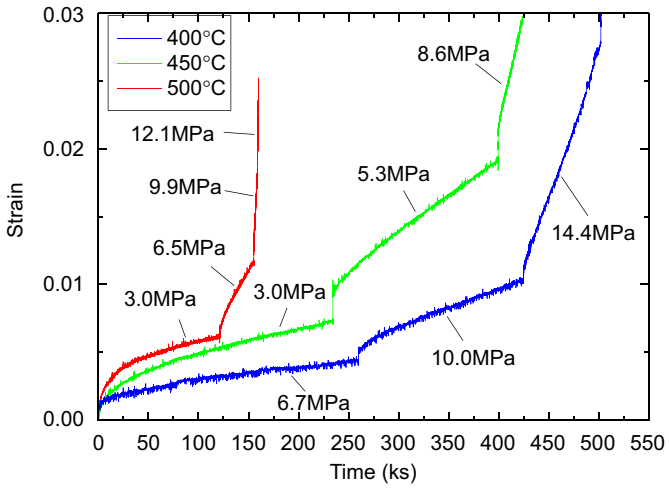

Fig. 3. Creep strain vs. time curves of cast Bi_2Te_3 at 400, 450 and 500 °C.

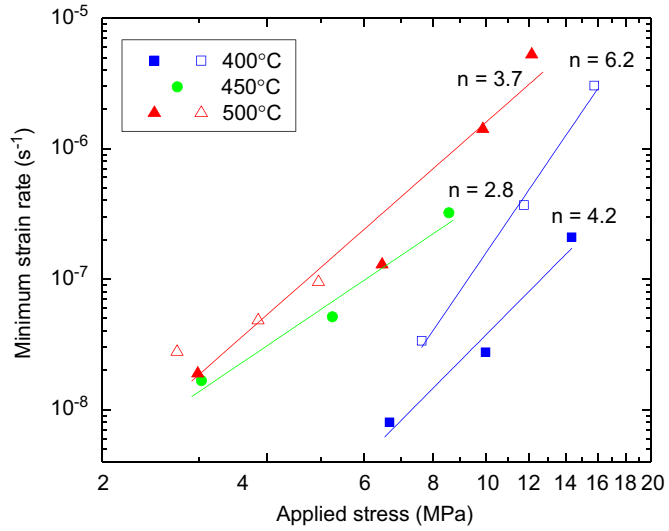

Fig. 4. Double logarithmic plot of minimum creep rate at 400, 450 and 500 °C vs. applied stress for cast Bi_2Te_3.

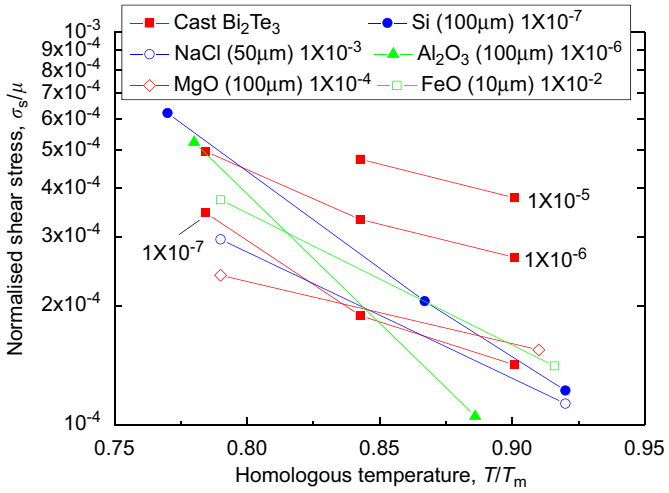

Fig. 5. Plot of normalized shear stress vs. homologous temperature at various strain rates for cast Bi_2Te_3 and other compounds (or element).

To compare compounds with different melting points, it is useful to normalize the shear stress σ_s by the shear modulus μ and to use the homologuous temperature T/T_m [11]. Fig. 5 shows the normalized shear stress, σ_s/μ vs. the homologous temperature, T/T_m, for Bi_2Te_3 and other materials [11] which exhibit ionic bonding, i.e., NaCl, Al_2O_3, MgO, FeO, and covalent bonding, i.e., Si. The shear modulus of Bi_2Te_3 was estimated from the relationship

$$\mu = \frac{E}{2(1+\nu)} \tag{2}$$

where E is the Young's modulus and ν is the Poisson's ratio. Due to the anisotropic properties of Bi_2Te_3, E ranges from 40 to 47 GPa and ν from 0.21 to 0.37 [8]. Taking average values $E=43$ GPa and $\nu=0.3$, a shear modulus $\mu=17$ GPa is calculated from Eq. (2). Each curve in Fig. 5 is related to a fixed shear strain rate, $\dot{\varepsilon}_s$. The shear stress, σ_s, and the shear strain rate, $\dot{\varepsilon}_s$, can be respectively calculated from the compressive uniaxial values based on simple relationships given in Ref. [11].

Compared with other materials in Fig. 5, coarse grained Bi_2Te_3 creeps more slowly under the same normalized shear stress (10^{-4}–10^{-3}) at the same homologous temperature (0.75–0.95). Thus, despite the poor strength of polycrystalline Bi_2Te_3 at ambient temperature due to early onset of failure from brittleness, this indicates that cast, coarse-grained Bi_2Te_3 shows high compressive creep resistance, even at high homologous temperatures and stresses. Thus, the weak bonding between the Te1–Te1 layers [4] does not lead to low creep strength, probably because dislocation glide necessitates slip on other planes with strong bonding as well. The grains in our cast samples, as shown in Fig. 2, are likely to be resistant against grain-boundary sliding and diffusional creep, as they are coarse, elongated and interwoven with each other.

Precipitates which improve the thermoelectric behavior by scattering phonons [12,13], may also reduce power-law creep rates by impeding dislocation motion. However, reducing grain size, which is also a strategy to improve thermoelectric properties [14], may lead to the onset of fast diffusional creep and may even trigger superplastic deformation. Furthermore, Bi_2Te_3 subjected to thermal cycling (e.g., during operation of thermoelectric modules under changing thermal loads) may show enhanced creep rates due to intergranular stresses resulting from the anisotropic coefficient of thermal expansion of Bi_2Te_3 [15–17].

3.3. Temperature dependence of creep rate

From Fig. 4, an estimate of the activation energy for steady-state creep, Q, can be calculated based on [18]

$$Q = -R_g \left[\frac{d \ln \dot{\varepsilon}}{d(1/T)}\right]_\sigma \tag{3}$$

For an applied stress of 8.5 MPa, Eq. (3) provides an activation energy, $Q=145$ kJ/mol between 400 and 500 °C ($T/T_m=$ 0.78–0.90). This activation energy value has high uncertainty, given the relatively narrow range of temperature and given that only four data points were used (removing one or the other data point at 400 °C provides $Q=117$ or 167 kJ/mol, illustrating the high uncertainty of the average Q value). Table 1 lists the creep activation energy of other covalent and ionic compounds (or element) shown in Fig. 5 [19]. As expected from Bi_2Te_3 having the lowest melting point, the activation energy of Bi_2Te_3 is the lowest.

3.4. Creep anisotropy

As shown in Fig. 4, there is strong variation in creep strain rates between specimens tested at the same temperature and stress, especially at 400 °C. This may be the result of testing Bi_2Te_3 with large grains which show creep anisotropy, i.e., some crystallographic orientations are stronger than others, as expected from the fact that Bi_2Te_3 has high crystallographic anisotropy leading to strong orientation dependence of, e.g., coefficient of thermal expansion and Young's modulus [20,21]. To test this hypothesis, compressive creep should be conducted on single crystals of known orientation, which is beyond the scope of the present study. In addition, it is apparent from Fig. 2 that grains exhibit a complex layered sub-structure, which may affect the motion of

Table 1
Activation energy of Bi_2Te_3 and other compounds (or element).

Materials	T/T_m	Q (kJ/mol)
Bi_2Te_3	0.78–0.90	145
Si	0.75–0.94	164
NaCl	0.75–0.95	203
Al_2O_3	0.7–0.9	482
MgO	0.48	212
FeO	0.73–0.95	328

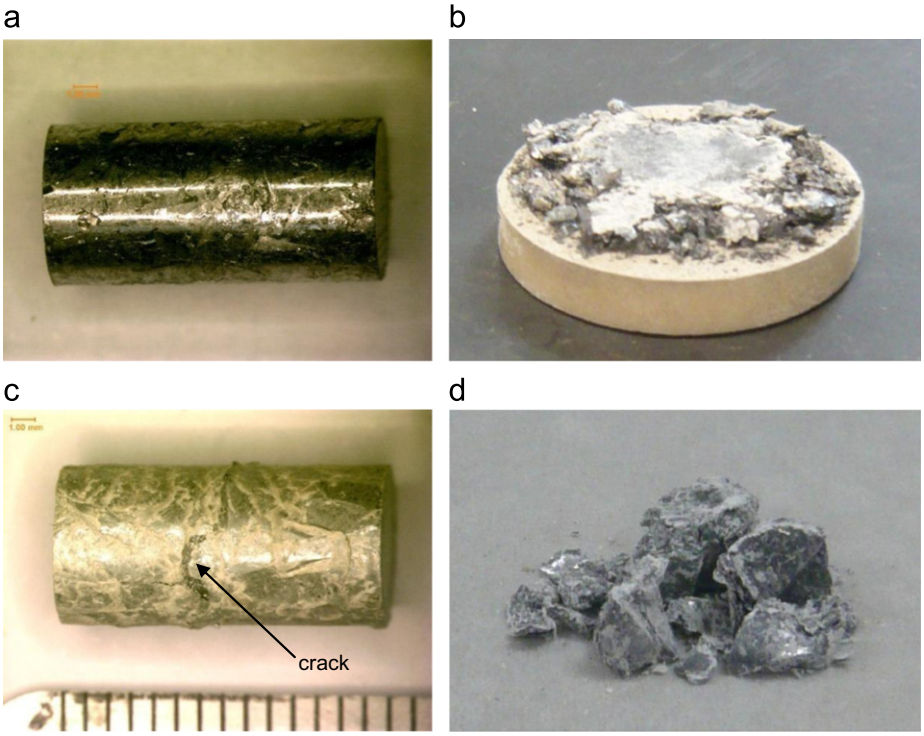

Fig. 6. Photographs of original specimen of cast Bi_2Te_3 and specimens fractured at 400, 450 and 500 °C: (a) original specimen of cast Bi_2Te_3; (b) specimen ruptured catastrophically into a large number of small fragments at 400 °C after creep strain of nearly 3%; (c) specimen keeping near-perfect shape except a long crack at 500 °C after creep strain of nearly 3% and (d) specimen ruptured much into a small amount of fragments which remained load-bearing at 450 °C after creep strain of nearly 3%.

dislocations gliding or climbing parallel or perpendicular to these layers. Finally, the creep behavior may be affected by defects in specimens (e.g., microcracks and casting porosity), which may vary along the length of the cast ingot, and among cast ingots. A follow-up study using a large number of well-defined specimens, both poly- and monocrystalline, may shed light on these questions.

3.5. Compressive fracture

When creep strain reached ~3%, specimens under compressive stresses at 400, 450 and 500 °C presented different fracture modes. The specimen at 400 °C ruptured catastrophically into a large number of small fragments as shown in Fig. 6(b). The specimen at 450 °C also ruptured in a brittle manner, but under the applied stress, much fewer fragments were created and they remained load-bearing, as shown in Fig. 6(d), indicating that the toughness may have increased somewhat at 450 °C. The specimen deformed at 500 °C displayed a nearly cylindrical shape, except for a long crack near the middle of the specimen, as shown in Fig. 6(c), indicating a higher level of plasticity than at 400 and 450 °C. This confirms prior reports that it is possible to shape Bi_2Te_3 by hot forging or hot extrusion, which may improve thermoelectric properties and mechanical properties of the material [22–25]. However, we note that the specimen deformed at 500 °C was tested under Ar, while those deformed at 400 and 450 °C were deformed in air, and might thus have become embrittled, e.g. due to grain-boundary oxidation.

4. Conclusions

The present study investigates the compressive creep behavior of cast Bi_2Te_3, which is relevant to the reliability of thermoelectric devices operating for long times under internal or external stresses, and to the hot forming (extruding and forging) of this material. Cast, coarse-grained Bi_2Te_3 shows high compressive creep resistance as compared to other covalent and ionic compounds at the same homologous temperature. For uniaxial compressive stresses between 2 and 16 MPa and temperatures between 400 and 500 °C, the minimum strain rate can be characterized by a power-law, with stress exponent with $n=3$–6 typical of most binary compounds, and an activation energy of ~145 kJ/mol. The strain rate can vary significantly from sample to sample for given stress and temperature conditions, which may be due to high creep anisotropy, with some crystallographic orientations stronger than others. In compression, Bi_2Te_3 fails in a brittle manner at 400 and 450 °C, but it shows compressive plasticity at 500 °C.

Acknowledgments

The authors thank Peter Bocchini, Mike Rawlings and Peiqi Zheng (Northwestern University) for experimental assistance. ZPG also acknowledges a fellowship from the CSC and the National Natural Science Foundation of China (No. 51005098) used to visit and do research at Northwestern University.

References

[1] T.M. Tritt, M.A. Subramanian, MRS Bull. 31 (2006) 188–194.
[2] H.J. Goldsmid, Bismuth—The thermoelectric material of the future, in: Proceedingsof the XXV International Conference on Thermoelectrics, ICT'06, 2006, pp. 5–10.
[3] S.B. Riffat, X.L. Ma, Appl. Therm. Eng. 23 (2003) 913–935.
[4] M.H. Francombe, Br. J. Appl. Phys. 9 (1958) 415–417.
[5] C.B. Satterthwaite, R.W. Ure, Phys. Rev. 108 (1957) 1164–1170.
[6] W.C. Wang, Y.L. Chang, Strain 47 (2011) 232–237.
[7] J. Gao, Q. Du, X. Zhang, et al., J. Electron. Mater. 40 (2011) 884–888.
[8] K. Biswas, M.S. Good, K.C. Roberts, et al., J. Mater. Res. 26 (2011) 1827–1835.
[9] S.N. Chizhevskaya, T.E. Svechnikova, N.M. Volkova, Inorg. Mater. 22 (1986) 806–809.

[10] J. Lee, A. Berger, L. Cagnon, et al., Phys. Chem. Chem. Phys. 12 (2010) 15247–15250.
[11] J.J. Frost, M.F. Ashby, Deformation-Mechanism Maps: The Plasticity and Creep of Metals and Ceramics, Pergamon, New York, 1982.
[12] K. Biswas, J. He, I. Blum, et al., Nat. Chem. 489 (2012) 414–418.
[13] C.J. Vineis, A. Shakouri, A. Majumdar, et al., Adv. Mater. 22 (2010) 3970–3980.
[14] A.J. Minnich, M.S. Dresselhaus, Z.F. Ren, et al., Energy Environ. Sci. 2 (2009) 466.
[15] C. Schuh, D.C. Dunand, Acta Mater. 50 (2002) 1349–1358.
[16] M.Y. Wu, J. Wadsworth, O.D. Sherby, Metall. Trans. A 18 (1987) 451.
[17] K. Kitazono, E. Sato, K. Kuribayashi, Scr. Mater. 44 (2001) 2695.
[18] M.E. Kassner, M.T. Perez-Prado, Prog. Mater. Sci. 45 (2000) 1–102.
[19] J.P. Poirier, Plasticité à haute température des solides cristallins, Eyrolles, Paris, 1976.
[20] V.T. Bublik, A.I. Voronin, E.A. Vygovskaya, et al., Inorg. Mater. 47 (2011) 1563–1568.
[21] J.J. Shen, L.P. Hu, T.J. Zhu, et al., Appl. Phys. Lett. 99 (2011).
[22] J.J. Shen, Z.Z. Yin, S.H. Yang, et al., J. Electron. Mater. 40 (2011) 1095–1099.
[23] R. Srinivasan, N. Gothard, J. Spowart, Mater. Lett. 64 (2010) 1772–1775.
[24] Z.C. Chen, K. Suzuki, S. Miura, et al., Mater. Sci. Eng. A 500 (2009) 70–78.
[25] T. Hayashi, Y. Horio, H. Takizawa, Mater. Trans. 51SI (2010) 1914–1918.